Dielectrophoretic manipulation of finite sized species and the importance of the quadrupolar contribution

Enzhu Liang,[1] Rosemary L. Smith,[1,2] and David S. Clague[3,*]
[1]*Department of Electrical Engineering, University of California, Davis, 1 Shields Ave., Davis, California 95616, USA*
[2]*Laboratory for Surface Science and Technology, University of Maine, 5764 Sawyer Research Center, Orono, Maine 04469-5764, USA*
[3]*Center for Micro and Nano Technology, L-223, Lawrence Livermore National Laboratory, Livermore, California 94551, USA*
(Received 8 September 2004; published 17 December 2004)

Dielectrophoresis (DEP) is the movement of polarizable species in a nonuniform electric field. DEP is used to attract (positive DEP) to or repel from (negative DEP) regions of high field intensity and is useful for manipulating species, including biological species. Current theoretical and numerical approaches used to predict the response to DEP forces assume that the target species is a point particle; however, in practice, the target species is of finite size, e.g., macromolecules, spores and assay beads. To elucidate the importance of target species size effects, higher order terms in the DEP force multipole expansion must be considered [P.R.C. Gascoyne and J. Vykoukal, Electrophoresis **23**, 1973 (2002)]. In this paper, we used the method of Green's function to derive and explore the importance of the quadrupolar contribution to the DEP forces acting on finite-sized species produced by a planar, interdigitated array of electrodes. Based on the analysis, it was found, for example, that at a fixed height of 20 μm in an interdigitated DEP array with an electrode width and spacing of 20 μm energized by a 10 Vp p, 1.0 MHz ac signal, the quadrupolar contribution to the total DEP force was 5% for a latex bead with 4.2 μm in radius and 10% for the one with 6 μm in radius. For a fixed, fractional quadrupolar contribution, β, both the exact calculation and the scaling estimate elucidate that the critical size of particle increase linearly with the electrode width (and spacing) at a fixed height, while the critical particle radius increases with a square-root dependence on the width height above the electrode in the electrode array.

DOI: 10.1103/PhysRevE.70.066617 PACS number(s): 41.20.−q, 87.50.Rr, 46.25.Cc, 89.75.Da

I. INTRODUCTION

Dielectrophoresis (DEP), termed by Pohl [1], is the movement of polarizable species in a nonuniform electric field to regions of high or low electric field, depending on the particle polarizability compared to the suspending medium (see also [2]). DEP has been used to effectively manipulate a wide range of biological species such as healthy and cancerous cells, DNA from lysate, bacteria and viruses, for different purposes, for examples, separation [3–5], detection [6], characterization [7], position and orientation [8,9]. Current theoretical and numerical methods that are widely used to predict the DEP forces use the dipole representation of the DEP force, which assumes that the target species are point particles. However, in practice, the target species are of finite sizes, e.g., macromolecules, spores and assay beads.

The typical time-average expression for conventional dielectrophoretic force based on dipole approximation as given by [10,11]

$$\underline{F}_{\mathrm{DEP}} = 2\pi\varepsilon_m a^3 \mathrm{Re}[f_{\mathrm{cm}}]\underline{\nabla}|\underline{E}_{\mathrm{rms}}\cdot\underline{E}_{\mathrm{rms}}|, \qquad (1)$$

where E_{rms} is the root mean square (rms) magnitude of the electric field, a is the radius of the particle, and ε_m is the real part of the complex permittivity of the suspending medium. The Clausius-Mossotti factor, $f_{\mathrm{cm}}=(\varepsilon_p^*-\varepsilon_m^*)/(\varepsilon_p^*+2\varepsilon_m^*)$, is the polarizability of the target species relative to the suspending fluid medium. ε_p^* and ε_m^* are the frequency dependent complex permittivities of the species and the suspending medium, respectively. The ability to manipulate suspending fluid properties and the frequency dependency enables the practitioner of DEP to preferentially separate desired species in different frequency ranges.

When performing analysis of DEP phenomena, it is, in general, highly desirable to have analytic expressions for the resultant fields produced by the electrode configuration; however, in practice, it is recognized that many electrode configurations are complicated, for example, a spiral electrode array [12] and do not lend themselves to closed form solutions. As a consequence, they often require numerical methods of investigation. To enable analytic expressions and order of magnitude estimates, we perform our analysis on a planar array of interdigitated electrodes, which is an amenable electrode configuration that permits closed form analytic expressions [13,14].

Morgan *et al.* [13] used Fourier analysis to obtain analytical expressions for the dipolar contribution to the DEP forces produced by an interdigitated electrode array that is valid when the levitation is greater than or equal to the electrode width. Alternatively, Wang *et al.* [11] derived a 3D Green's function that is dependent on the surface potential using the method Green's second identity to relate the desired potential field produced by a surface potential to a known, appropriately chosen auxiliary function, see [11] for details. Later, Clague and Wheeler [14] used the 2D upper-half-plane Green's function, which was functionally different from Wang's resultant Green's function; however, both approaches yielded the identical results for the potential field produced by a 2D array of parallel electrodes. These methods produce

*Corresponding author. Email address: clague1@llnl.gov

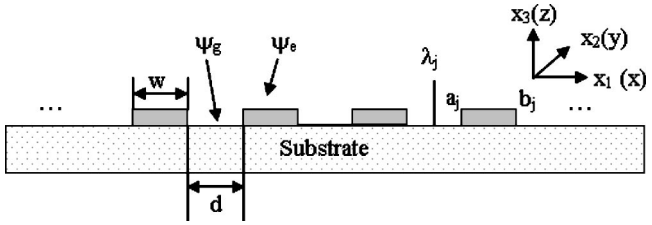

FIG. 1. Interdigitated DEP electrode array. Four electrodes are shown to illustrate electrode positioning and important geometric parameters.

useful results and are computationally more efficient than standard numerical methods [11]. In all three of these efforts, however, they restricted their analysis to the dipole approximation of the DEP force.

Analytic approaches for predicting the dependence of DEP forces on species size and higher order field effects considering the size and high order field effects have been proposed in the literature [15–18]; however, all these methods assume that the electric field and its derivatives are known and therefore, analytical solutions to the electric field are necessary to explore the importance of higher order effects.

In this paper, we use the method of Green's functions and derive an analytical solution to the electric field produced by an interdigitated DEP electrode array. By combining the resultant expression for the electric field with the general DEP force formulation by Jones [17], we derive the desired expressions for the quadrupolar contribution and perform a study to elucidate the importance of the quadrupole contribution to the DEP force as a function of system parameters, e.g., length scales.

The remainder of the paper is divided into the following sections: in Sec. II we review the theory and derive the necessary expressions for the dipole and quadrupole contributions to the DEP force; in Sec. III we perform studies to show the contribution of the quadrupole to the DEP force relative to the dipole representation. In Sec. III A, we give a comparison of the field and its derivatives; in Sec. III B, a validation of the theory is given by comparing to the previous reports; in Secs. III C and III D, we explore quadrupolar contribution as a function of target-species size and height above plane of the electrode array plane; in Sec. III E, we combine the size and height effect and develop a scaling estimate to permit a rapid prediction of the conditions when the quadrupolar contribution becomes significant.

II. THEORY

In this work, we start with and extend the result of Clague and Wheeler [14]. They use the upper-half-plane Green's function and a linear approximation for the surface potential in the gaps [11] between electrodes to predict the gradient in the electric field strength for the approximation of the conventional DEP force (standing wave) produced by a array of parallel electrodes, i.e., interdigitated electrode configuration shown in Fig 1.

The electrode width is w and the gap or spacing between the electrodes is d. The leading and trailing edges of the jth electrode are given by a_j and b_j, respectively. λ_j represents the midpoint between the jth pair of electrodes. ψ_g and ψ_e are the potentials of the electrodes and gaps, respectively.

Using the approach of Wang *et al.* [11] and Clague *et al.* [14], the electric potential above the electrode array given in Fig. 1 is given by

$$\psi(x,z) = -\frac{1}{\pi}\sum_{j=1}^{N}\psi_e\left(\arctan\left[\frac{x-b_j}{z}\right]-\arctan\left[\frac{x-a_j}{z}\right]\right) - \frac{1}{\pi}\sum_{j=1}^{N-1}\psi_g(x)\left(\arctan\left[\frac{x-a_{j+1}}{z}\right]-\arctan\left[\frac{x-b_j}{z}\right]\right) + \frac{1}{\pi}\sum_{j=1}^{N-1}\frac{C_2}{2}z\ln\frac{z^2+(x-a_{j+1})^2}{z^2+(x-b_j)_2}. \quad (2)$$

Here z is the height of the particle above the surface of the electrode array, and x lateral position along the array; C_2 is the coefficient in the gap potentials. The electric field is determined by taking the negative gradient of the potential, Eq. (2), or

$$\underline{E}(x,z) = -\underline{\nabla}\psi(x,z). \quad (3)$$

By taking the gradient of Eq. (3), one can construct the desired expressions to approximate the dipolar contribution to the DEP force, Eq. (1). We, however, are interested in extending this result to include the quadrupolar contribution to the force.

The general expression, as given by Jones [17], for the time-averaged DEP force including both dipolar and quadrupolar contributions has the following form:

$$F_{\mathrm{DEP}} = 2\pi\varepsilon_m\left\{K^{(1)}a^3\underline{\nabla}(\underline{E}\cdot\underline{E}) + \frac{K^{(2)}a^5}{3}\underline{\nabla}(\underline{\nabla}\underline{E}:\underline{\nabla}\underline{E}) + (\text{higher-order terms})\right\}. \quad (4)$$

Here $K^{(n)}=(\varepsilon_p^*-\varepsilon_m^*)/[n\varepsilon_p^*+(n+1)\varepsilon_m^*]$ is the generalized species polarizability, which permits the inclusion of higher order moments, n, being related to the order of the contribution from the multipole expasion. ε_p^* and ε_m^* are again the frequency dependent complex permittivities of the particle and suspending medium, respectively. The first term on the right of Eq. (4) is the dipole contribution, which is shown in Eq. (1) and the second term on the right-hand side is the quadrupolar contribution to the DEP force.

To assess the importance of the quadrupolar contribution to the DEP force, we simply determine what percent, β, of the total force the quadrupole represents:

$$\beta \leqslant \frac{|F_Q|}{|F_T|}\times 100\% = \frac{|a^2\underline{\nabla}(\underline{\nabla}\underline{E}:\underline{\nabla}\underline{E})|}{\left|3\frac{K^{(1)}}{K^{(2)}}\underline{\nabla}(\underline{E}\cdot\underline{E}) + a^2\underline{\nabla}(\underline{\nabla}\underline{E}:\underline{\nabla}\underline{E})\right|}\times 100\%. \quad (5)$$

Here F_Q is the quadrupolar contribution only and F_T is the

total DEP force (e.g., the dipolar plus quadrupolar contributions to the DEP force). If we chose a tolerance, β, for when it is advisable to include the quadrupolar term, say, when $\beta \sim 5\%$, then we can better understand the important parameters that govern DEP particle manipulation, e.g., the critical particle size and height above the electrode array. While the excitation voltage, applied field frequency and Clausius-Mossotti factor play an important role to the force ratio described in Eq. (5), we are primarily concerned with the electric field intensity and the associated gradients. The quadrupolar contribution has the following form:

$$\underline{F}_Q = 2\pi\varepsilon_m \frac{K^{(2)}a^5}{3} \underline{\nabla}(\underline{\nabla}\underline{E}:\underline{\nabla}\underline{E}). \tag{6}$$

When using index notation, Eq. (6) can be expanded as

$$\underline{\nabla}(\underline{\nabla}\underline{E}:\underline{\nabla}\underline{E}) = \Sigma_k \underline{\delta}_k \left\{ \Sigma_i \Sigma_j \left(\frac{\partial E_j}{\partial x_i} \frac{\partial^2 E_i}{\partial x_k \partial x_j} + \frac{\partial E_i}{\partial x_j} \frac{\partial^2 E_j}{\partial x_k \partial x_i} \right) \right\} \times (i = 1,2,3;\ j = 1,2,3;\ k = 1,2,3), \tag{7}$$

where E_1, E_2, E_3 are components of the electric field. The indices 1, 2, 3 are equivalent to x, y, z in the Cartesian coordinates and $\underline{\delta}_k$ is the unit vector in k direction (k=1,2,3). However, in the x_2 *or* y direction, that is along the electrode, ignoring end effects, the electric field is considered constant and therefore all the x_2 components are zero. To quantify the quadrupolar contribution, all the components $\{\partial E_j/\partial x_i,\ \partial^2 E_i/\partial x_k \partial x_j\}$ must be found explicitly. However, the following quantities are equivalent:

$$\frac{\partial E_x}{\partial z} = \frac{\partial E_z}{\partial x}, \quad \frac{\partial^2 E_x}{\partial x \partial z} = \frac{\partial^2 E_z}{\partial x^2}, \quad \frac{\partial^2 E_z}{\partial x \partial z} = \frac{\partial^2 E_x}{\partial z^2}. \tag{8}$$

Therefore, if one derives expressions for E_x, E_z, $\partial E_x/\partial x$, $\partial E_x/\partial z$, $\partial E_z/\partial z$, $\partial^2 E_x/\partial x^2$, $\partial^2 E_x/\partial x \partial z$, $\partial^2 E_z/\partial x \partial z$, and $\partial^2 E_z/\partial z^2$, the field related contributions to dipole and quadrupole DEP forces are fully specified. The equivalence of the terms given in Eq. (8), which complete the list of necessary expressions to predict the quadrupolar force contributions, was confirmed and validated via using symbolic mathematics packages, e.g., Mathematica® (Wolfram Research). The electric fields and first partials of the electric fields shown above have been derived previously [14], and the remaining second partials are given in the Appendix.

III. RESULTS AND DISCUSSIONS

The particles subject to DEP forces produced by an interdigitated electrode array can be either attracted (positive DEP) to or repelled from (negative DEP) regions of high field strength, i.e., at the electrode edges for the configuration under consideration. Positive or negative DEP is determined by the sign of the relative difference between the complex permeabilities of the target species and the suspending medium. The force is also a function of the particle size, electrode width, spacing between electrodes and height above the electrode array.

In the subsections to follow, we present and compare the electric field intensities (and gradients in the electric field intensities) for the dipole and quadrupole contributions to the DEP force, identify a critical particle size that gives rise to a specific β and quantify particle height effects relative to the electrode array and explore the coupled particle size and height effects. For all of the studies, we consider an electrode array with equal width, w, and spacing, d, fixed at 20 μm and the magnitude of the applied voltage signal is 10 $V_{p\text{-}p}$ with 180° phase shifts between adjacent electrodes operating at a frequency of 1.0 MHz unless another signal is specified.

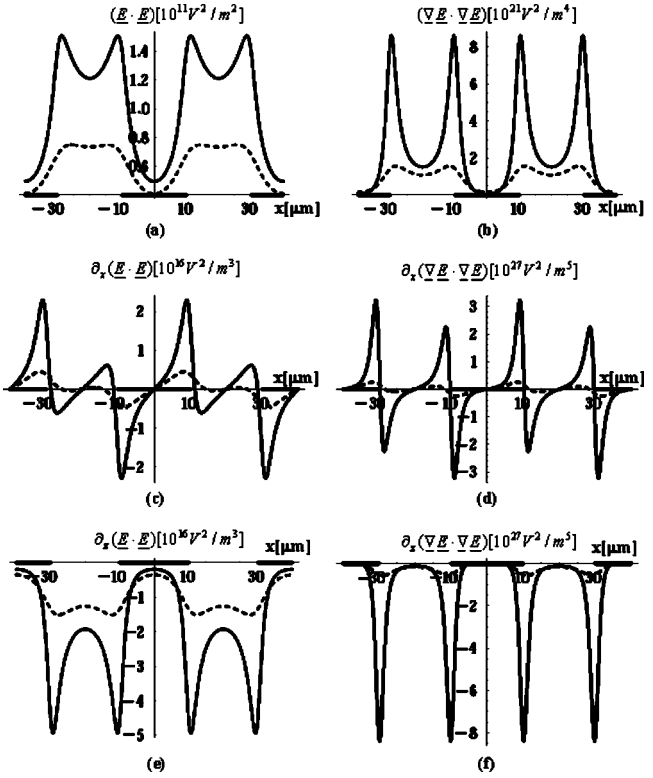

FIG. 2. The contributions to the DEP force from $(\underline{E}\cdot\underline{E})$, $(\underline{\nabla}\underline{E}:\underline{\nabla}\underline{E})$ and their associated gradients in components form as a function of horizontal position along the electrode array at fixed vertical positions of 2 μm (solid curves) and 5 μm (dash curves). The interdigitated electrode array consists of 20 μm wide electrodes with spacing equal to the width and is energized by a 10 $V_{p\text{-}p}$, 1.0 MHz AC signal. The short, black, thicker horizontal lines represent the electrodes.

A. Electric field and gradients in the electric field intensities

The DEP force is generated by the gradient in electric field intensity, $(\underline{E}\cdot\underline{E})$, for the dipolar term and the gradient of the scalar product of the gradient field intensity, $(\underline{\nabla}\underline{E}:\underline{\nabla}\underline{E})$, for the quadrupolar term. To get better understand the importance of the quadrupolar contribution, we compare $(\underline{E}\cdot\underline{E})$, $(\underline{\nabla}\underline{E}:\underline{\nabla}\underline{E})$ and their associated derivatives in x and z directions at two different heights of 2 μm and 5 μm above the electrode array as a function of position along the electrode array; see Figs. 2(a)–2(f).

The shapes of the contributions are indeed similar to each other when plot as a function of x position at fixed heights.

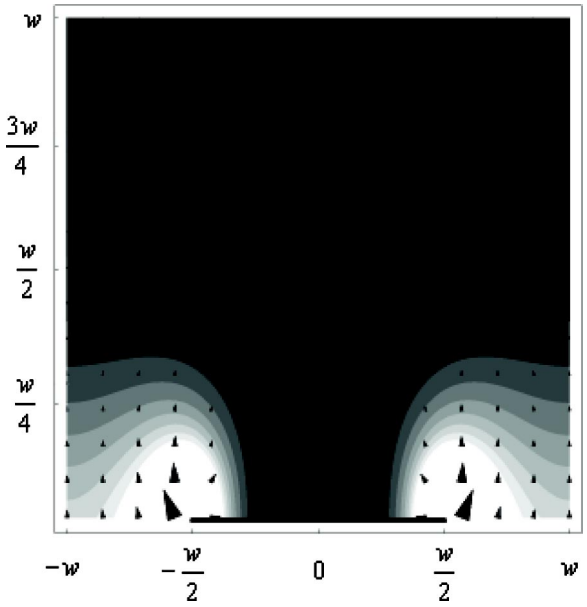

FIG. 3. DEP force field, including the quadrupole contribution to the force prediction, produced by an interdigitated DEP array energized by an ac signal. The electrode width and the spacing between two adjacent electrodes are equal and represented by *w*; the short, black line represents one of the electrodes. The gray scale is from maximum force (white) close to the electrode edges to the minimum (black) and the arrows designate the force directions.

However, the contribution from $(\underline{\nabla E}:\underline{\nabla E})$ is approximately 10 orders of magnitude greater than the contribution from the electric field intensity $(\underline{E}\cdot\underline{E})$. The *x* and *z* component of the gradient of the quantities are shown in Figs. 2(c)–2(f), respectively and as expected, the maxima happen at the electrode edges. However, contributions resulting from the components of $\underline{\nabla}(\underline{\nabla E}:\underline{\nabla E})$ are approximately 11 orders of magnitude greater than those from $\underline{\nabla}(\underline{E}\cdot\underline{E})$ at the same position. As expected, the magnitude of the gradients increase exponentially as the particle approaches the electrode plane. Because, the quadrupolar contribution to the overall DEP force is proportional to the square of the particle radius relative to the dipolar contribution, see Eq. (4) and Eq. (5), the quadrupolar contribution becomes increasingly important as the radius increases and as the particle approaches the electrode surface.

Figure 3 combines a vector plot and a contour plot to show the predicted DEP force field, including the quadrupole contribution, produced by an interdigitated electrode array in which the electrode width is equal to the spacing.

Qualitatively, the quadrupolar contribution does not alter the general features of the DEP force field [11,14], meaning that the strongest forces still happen at the edges of the electrodes and the components in horizontal *x* direction are comparable to the ones in vertical *z* direction; while the *z* components in *z* direction become dominant as the level goes higher.

B. Validation of theory: Comparison to previous reports

Morgan *et al.* derived an analytical solution for levitation heights produced by an interdigitated electrode array using Fourier series analysis [13] and Markx *et al.* carried out experiments to determine the levitation heights of different size latex beads produced by interdigitated electrode arrays with various electrode widths (spacings) [19]. The theoretical results of Moran *et al.* [13] agreed well with Markx *et al.* [19].

To validate our analytic expressions, we compare our results with the theoretical results of Morgan *et al.* [13] and the experimental results of Markx *et al.* [19] by predicting the DEP force and levitation heights using the same system parameters, i.e., for a 6 μm latex bead that has a conductivity of 0.65×10^{-7} S/m and a relatively dielectric constant of 5.5 and that is suspended in a suspending medium that has a conductivity of 1.1 mS/m and a relatively dielectric constant of 79. Given these parameters at a frequency of 1.0 MHz, the real parts of $K^{(1)}$ and $K^{(2)}$ are −0.478 and −0.317, respectively, meaning that a levitation force (negative DEP) will balance sedimentation or gravitational force and the particles will achieve an equilibrium levitation height. In Table I, we compare our results with those of Morgan *et al.* and Markx *et al.*

In each comparison the radius of the latex particle was taken as 3 μm, and the electrode width/spacing, 20 μm. h_0 represents the levitation heights from our prediction. The two entries for h_0 represent the levitation height predicted using the dipole and the dipole plus the quadrupole contributions. There h_1 and h_2 are theoretical and experimental results from previous papers [13,19], respectively. As shown in Table I, the agreement is excellent validating the accuracy of our analytic expressions. As is seen, when the levitation heights are

TABLE I. Levitation height comparisons with previously published results. (All the heights in Table I are in microns.)

	$V_0=2\ V_{p\text{-}p}$			$V_0=6\ V_{p\text{-}p}$			$V_0=8\ V_{p\text{-}p}$		
Electrode width and spacing (μm)	h_0(theory) (this work)	h_1(theory) [13]	h_2(exp) [19]	h_0(theory) (this work)	h_1(theory) [13]	h_2(exp) [19]	h_0(theory) (this work)	h_1(theory) [13]	h_2(exp) [19]
40	74.8	70	72	85.4	80	82	92.3	88	92
	74.9			85.7			92.3		
20	49.9	48	50	55.1	55	55	58.8	62	59
	51.1			55.3			59.0		
10	32.0	35	32	34.6	40	34			
	32.2			35.0					

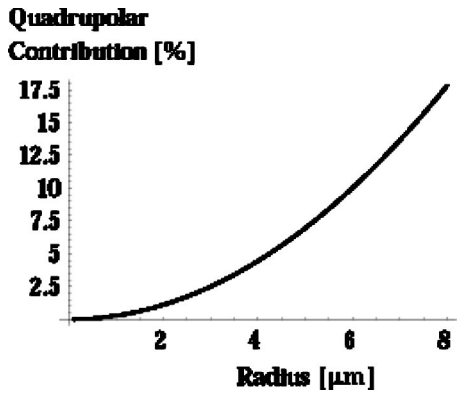

FIG. 4. Plot of the quadrupolar contribution to the total DEP force as a function of the latex bead radius. The bead is fixed at the height of 20 μm. The electrode width and spacing are 20 μm, respectively, and the array is energized by a 10 $V_{p\text{-}p}$, 1.0 MHz ac signal.

greater than the electrode width and spacing, the quadrupole contribution is negligible. In the subsections to follow, the significance of the quadrupolar contribution is determined by the combination of the levitation height, for when the height is less than or equal to the electrode width, and particle size.

C. Target species size effects

As shown in Eq. (4), the particle size effect is an important factor when considering the quadrupolar contribution. Figure 4 shows the % contribution of the quadrupole as a function of the particle radius at a fixed height of 20 μm above an interdigitated DEP array with an electrode width and spacing of 20 μm energized by a 10 $V_{p\text{-}p}$, 1.0 MHz ac signal using the physical properties for latex beads.

As shown in Fig. 4, the fractional quadrupolar contribution exhibits a quadratic dependence on the radius of the bead, which is predicted in Eq. (5).

For this particular electrode configuration, the quadrupolar contribution is 2.5% for a radius of 3.0 μm of the total force, 5% for a radius of 4.2 μm and 10% for a radius of 6.0 μm. However, for the 6 μm latex beads (3 μm in radius) used in the validation session, the variation should be much less than 2.5% since the levitation height is much higher than 20 μm and this explains why we did not see the quadrupolar contribution in Table I.

D. Height effects

To explore the relative importance of the dipolar and quadrupolar contributions to the DEP force, we compare the magnitudes of the force contributions, i.e.,

$$F_i = \sqrt{F_{xi}^{\,2} + F_{zi}^{\,2}} \quad \text{with} \begin{cases} i = D: & \text{dipole contribution,} \\ i = Q: & \text{quadruple contribution,} \\ i = T: & \text{total contribution.} \end{cases} \tag{9}$$

As suggested in the electric field nonuniformity plots in Fig. 2, the quadrupolar contribution becomes more and more important when the particles get closer to the electrode surface. In Fig. 5, we plot the DEP forces contributed by dipolar and dipolar plus quadrupolar terms varying with levitation heights for 6 μm latex beads at the electrode edges, where the force is strongest.

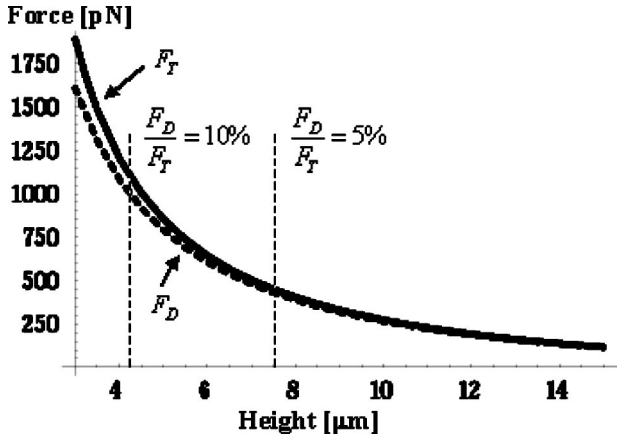

FIG. 5. DEP forces acting on a 6 μm latex bead predicted using the combined dipole plus quadrupole terms (F_T) is compared to the force predicted using only the dipole term only (F_D) compared as a function of levitation heights above an interdigitated DEP array. The electrode width and spacing are both 20 μm and the array is energized by a 10 $V_{p\text{-}p}$, 1.0 MHz ac signal. The force estimates were assessed at an electrode edge, where the force is at a maximum.

The test heights above the array ranged from 3 μm to 15 μm for the same interdigitated electrode configuration array.

The two curves approach to each other and finally overlap as the height increases. Additionally, both forces decrease exponentially with the levitation height. In this specific case, the quadrupolar contribution to the force drop to less than 10% at the height of 4.5 μm and less than 5% at 7.5 μm.

To explore the DEP force field beyond electrode edges, Fig. 6 we contrast the magnitude of the DEP forces predicted by the dipolar plus quadrupolar terms versus the dipolar term alone as a function of position along the electrode array at fixed, test heights of 6 μm and 15 μm, respectively.

The forces experienced by the test particle closer to the electrode surface have spikes at the electrode edges and a wide range of magnitude from 200 pN to 700 pN, while the forces experienced by the test particle far from the electrode surface are spatially more uniform varying in a smaller range from 95 pN to 130 pN.

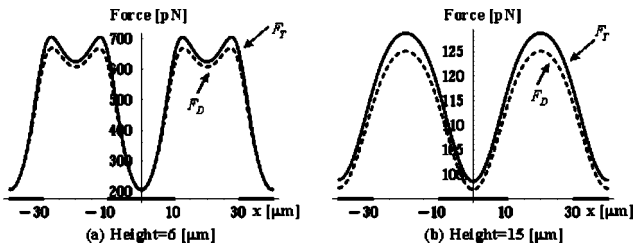

FIG. 6. Comparison of the magnitude of the DEP force acting on a 6 μm latex bead as predicted by the dipole plus quadruple and dipole alone as a function of horizontal position along the electrode array at fixed heights of 6 μm and 15 μm.

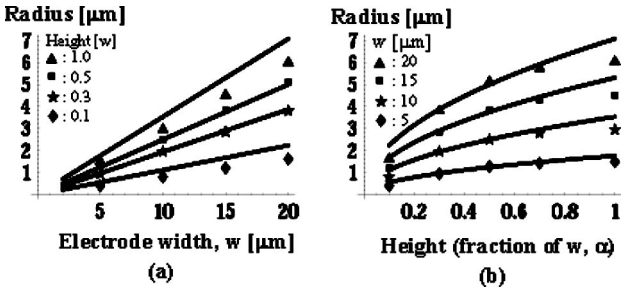

FIG. 7. The critical species radius, that is the radius that causes the quadrupolar contribution to be 10% of the total, predicted DEP force, as a function of electrode width (with spacing equal to the width) and target species height above the electrode array. In all numerical experiments, the electrode array was energized by 10 $V_{p\text{-}p}$, 1.0 MHz ac signals. For all test cases, the spacing is equal to the electrode width. The discrete data points represent the calculations based on the complete theory presented in this communication; see Eqs. (4) and (6)–(8), and the solid lines represent predictions based on the scaling estimate given in Eq. (13), for $\gamma=0.5$.

E. Combining electrode width, target species height, and size effects

The above discussion is based on an interdigitated DEP electrode array with a width and spacing of 20 μm energized by a 10 $V_{p\text{-}p}$, 1.0 MHz ac signal. In order to give intuition for variations in system parameters, e.g., electrode width, target species height and size effects, we solve the full set of equations and develop scaling estimates to predict the critical particle size for when quadrupolar contribution reaches a specified tolerance, β, see Eq. (5). In Figs. 7(a) and 7(b), the tolerance, β, is set to 10% and the critical particle radius is determined as a function of electrode width for fixed species heights above the electrode array.

Shown above in Fig. 7(a) is the critical particle size as a function of electrode width for fixed heights and a percentage of quadrupolar contribution of β of 10%. The discrete data points are from the critical species radii predicted from the full set of equations, and the lines are qualitative predictions from the scaling estimate. As shown above, the critical particle size increases linearly with an increase of electrode width at every height sampled. Also note that when the particle height is closer to the electrode array, $z=0.1$ w, that the critical particle radii range from submicron to ~ 3 μm. In contrast, as the particle moves vertically away from the electrode array, the critical particle size can be increased, in some cases substantially, to fall within the specified tolerance, β, 10% quadrupolar contribution to the overall DEP force. Additionally, as the electrode width increases and the vertical position increases, the critical particle size increases monotonically.

To elucidate this monotonic increase in critical particle size with increase in electrode width, in Fig. 7(b) we show the same data in a different perspective. The data show more dramatically that the dependence of critical particle size as a function of height for various electrode widths. As shown the crucial particle size exhibits a nonlinear dependence on height above the electrode array for a fixed electrode width.

This is clearly understood by doing the scaling estimate for the quadrupolar contribution using Eq. (5) and rewrite it based on a characteristic length scale, l, over which the electric field and electric field intensity changes:

$$\beta \sim \tilde{\mathrm{O}}\left(\frac{\left|a^5\frac{V^2}{l^5}\right|}{3\left|\frac{K^{(1)}}{K^{(2)}}a^3\frac{V^2}{l^3}+a^5\frac{V^2}{l^5}\right|}\right)=\tilde{\mathrm{O}}\left(\frac{\left|a^2\frac{1}{l^2}\right|}{3\left|\frac{K^{(1)}}{K^{(2)}}+a^2\frac{1}{l^2}\right|}\right), \tag{10}$$

V is the applied signal and if we let $K=K^{(1)}/K^{(2)}$, then we can rearrange to solve for the critical particle radius, a_c,

$$a_c \sim \tilde{\mathrm{O}}\left(\sqrt{\frac{3K\beta}{(1-\beta)}}l^2\right). \tag{11}$$

For convenience, we keep the characteristic length scale, l, under the radical. If $h \gg w$, then $l \sim h$, and if $w \gg h$ then $l \sim w$; however, when $w \sim h$, from the expressions given in the Appendix and as shown in the Appendix of Clague and Wheeler [14], we know that the characteristic length scales of the system involve both w and h. Therefore, if we write h in terms of w, $h=\alpha w$, where $0<\alpha \leqslant 1$, then l^2 can be expressed as αw^2 and Eq. (11) simplifies to

$$a_c \sim \tilde{\mathrm{O}}\left(w\sqrt{\frac{3K\beta}{(1-\beta)}\alpha}\right). \tag{12}$$

Here, α is the fractional prefactor on w for describing the particle height. To actually provide a useful correlation for quick estimates, we multiply the scaling estimate given in Eq. (12) by a constant, γ,

$$a_c = \gamma\left(w\sqrt{\frac{3K\beta}{(1-\beta)}\alpha}\right). \tag{13}$$

We fit the data with Eq. (13) to determine γ. For a constant height, Fig. 7(a), α is constant and a_c is expected to exhibit a linear dependence on w; however, if w is fixed and h is varied, it is expected, according to Eq. (13), that a_c will exhibit square-root dependence on h or on α is illustrated in Fig. 7(b).

For the specific case above, $\beta=10\%$ and $K=1.5$, a best-fit value for γ was found to be 0.5 and using this γ in Eq. (13) the scaling estimate was plotted with the more rigorous estimates as solid lines in both Figs. 7(a) and 7(b). As seen in the figure, the agreement is very good and therefore, the resulting scaling estimate provides a rapid way to determine under what circumstances DEP force estimates need to include the quadrupolar contribution. Additionally, if one chooses to neglect the quadrupolar contribution, Eq. (13) can be rearrange to give a quick and reasonable estimate of the expected error in DEP force predictions.

IV. CONCLUSION

In this paper we explore the importance of the quadrupolar contribution to the DEP force acting on finite sized species. To accomplish this, we used the method of Green's functions to develop an analytic expression for the DEP force on a spherical particle in a field produced by a planar array of

interdigitated electrodes that includes the quadrupolar contribution. It was shown that the quadrupolar contribution was indeed very important, i.e., the gradients in the field terms was ~11 orders of magnitude gradient in electric field intensity; therefore, given a particle of sufficient radius or proximity to the electrode array, the noninclusion of the quadrupolar contribution could result in an unacceptable amount of error in predictions of DEP forces. The rigorous analytic solution developed in this communication yields excellent agreement with previous reports as the particles are levitated far from the electrode surface [11,19]. Analytic solutions to all of the fields and associated gradients are provided in [14] and in the Appendix. A scaling estimate was derived to facilitate rapid prediction of critical particle size for when the quadrupolar contribution needs to be included, or in contrast this scaling estimate can be used to ascribe an error estimate to the DEP force calculation when using the dipole approximation. The scaling estimate reveals a linear dependence of the critical particle size at fixed height on electrode width. Also as the height is increased at fixed electrode width, the scaling estimate reveals a square-root dependence on height.

ACKNOWLEDGMENTS

This project was funded in part by DARPA/BioFLIPS Contract No. N66001-01-C-8001. This work was performed, in part, under the auspices of the U.S. Department of Energy by University of California, Lawrence Livermore National Laboratory under Contract No. W-7405-Eng-48.

APPENDIX

Equations for the second-order derivatives of the electric field:

$$\frac{\partial^2 E_x}{\partial x \partial x} = \frac{1}{\pi}\sum_{j=1}^{N} \psi_e \left(\frac{2z^3 - 6z(x-a_j)^2}{[z^2+(x-a_j)^2]^3} - \frac{2z^3 - 6z(x-b_j)^2}{[z^2+(x-b_j)^2]^3} \right) + \frac{1}{\pi}\sum_{j=1}^{N-1} \psi_g(x) \left(\frac{2z^3 - 6z(x-b_j)^2}{[z^2+(x-b_j)^2]^3} - \frac{2z^3 - 6z(x-a_{j+1})^2}{[z^2+(x-a_{j+1})^2]^3} \right) + \frac{1}{\pi}\sum_{j=1}^{N-1} 8C_2 z \left(\frac{(x-b_j)^3}{[z^2+(x-b_j)^2]^3} - \frac{(x-a_{j+1})^3}{[z^2+(x-a_{j+1})^2]^3} \right), \tag{A1}$$

$$\frac{\partial^2 E_x}{\partial x \partial z} = \frac{1}{\pi}\sum_{j=1}^{N} \psi_e \left(\frac{2(x-a_j)^3 - 6(x-a_j)z^2}{[z^2+(x-a_j)^2]^3} - \frac{2(x-b_j)^3 - 6(x-b_j)z^2}{[z^2+(x-b_j)^2]^3} \right) + \frac{1}{\pi}\sum_{j=1}^{N-1} \psi_g(x) \times \left(\frac{2(x-b_j)^3 - 6(x-b_j)z^2}{[z^2+(x-b_j)^2]^3} - \frac{2(x-a_{j+1})^3 - 6(x-a_{j+1})z^2}{[z^2+(x-a_{j+1})^2]^3} \right) + \frac{1}{\pi}\sum_{j=1}^{N-1} C_2 \left(\frac{3(x-a_{j+1})^4 - 6(x-a_{j+1})^2 z^2 - z^4}{[z^2+(x-a_{j+1})^2]^3} - \frac{3(x-b_j)^4 - 6(x-b_j)^2 z^2 - z^4}{[z^2+(x-b_j)^2]^3} \right), \tag{A2}$$

$$\frac{\partial^2 E_x}{\partial z \partial z} = \frac{1}{\pi}\sum_{j=1}^{N} \psi_e \left(\frac{2z^3 - 6z(x-b_j)^2}{[z^2+(x-b_j)^2]^3} - \frac{2z^3 - 6z(x-a_j)^2}{[z^2+(x-a_j)^2]^3} \right) + \frac{1}{\pi}\sum_{j=1}^{N-1} \psi_g(x) \left(\frac{2z^3 - 6z(x-a_{j+1})^2}{[z^2+(x-a_{j+1})^2]^3} - \frac{2z^3 - 6z(x-b_j)^2}{[z^2+(x-b_j)^2]^3} \right) + \frac{1}{\pi}\sum_{j=1}^{N-1} 8C_2 z \left(\frac{(x-a_{j+1})^3}{[z^2+(x-a_{j+1})^2]^3} - \frac{(x-b_j)^3}{[z^2+(x-b_j)^2]^3} \right), \tag{A3}$$

$$\frac{\partial^2 E_z}{\partial z \partial z} = \frac{1}{\pi}\sum_{j=1}^{N} \psi_e \left(\frac{2(x-b_j)^3 - 6(x-b_j)z^2}{[z^2+(x-b_j)^2]^3} - \frac{2(x-a_j)^3 - 6(x-a_j)z^2}{[z^2+(x-a_j)^2]^3} \right) + \frac{1}{\pi}\sum_{j=1}^{N-1} \psi_g(x) \times \left(\frac{2(x-a_{j+1})^3 - 6(x-a_{j+1})z^2}{[z^2+(x-a_{j+1})^2]^3} - \frac{2(x-b_j)^3 - 6(x-b_j)z^2}{[z^2+(x-b_j)^2]^3} \right) + \frac{1}{\pi}\sum_{j=1}^{N-1} C_2 \left(\frac{3(x-b_j)^4 - 6(x-b_j)^2 z^2 - z^4}{[z^2+(x-b_j)^2]^3} - \frac{3(x-a_{j+1})^4 - 6(x-a_{j+1})^2 z^2 - z^4}{[z^2+(x-a_{j+1})^2]^3} \right). \tag{A4}$$

[1] H. Pohl, *Dielectrophoresis* (Cambridge University Press, New York, 1978).
[2] P. R. C. Gascoyne and J. Vykoukal, Electrophoresis **23**, 1973 (2002).
[3] J. Yang, Y. Huang, X. Wang, X. B. Wang, F. F. Becker, and P. R. C. Gascoyne, Biophys. J. **76**, 3307 (1999).
[4] J. Yang, Y. Huang, X. B. Wang, F. F. Becker, and P. R. C. Gascoyne, Biophys. J. **78**, 2680 (2000).
[5] J. Yang, Y. Huang, X. B. Wang, F. F. Becker, and P. R. C. Gascoyne, Anal. Chem. **71**, 911 (1999).

[6] J. Suehiro, M. Shutou, T. Hatano, and M. Hara, *Sensors & Actuators B-Chemical* (Elsevier, Switzerland, 2003), Vol. B 96, no. 1-2, pp. 144–51.
[7] M. P. Hughes, H. Morgan, and F. J. Rixon, Biochim. Biophys. Acta **1571**, 1 (2002).
[8] F. Dewarrat, M. Calame, and C. Schönenberger, Single Mol. **3**, 189 (2002).
[9] W. A. Germishuizen *et al.*, Nanotechnology **14**, 896 (2003).
[10] T. B. Jones, *Electromechanics of Particles* (Cambridge University Press, Cambridge, England, 1995).
[11] X. Wang, X. B. Wang, F. F. Becker, and P. R. C. Gascoyne, J. Phys. D **29**, 1649 (1996).
[12] A. D. Goater, J. P. H. Burt, and R. Pethig, J. Phys. D **30**, L65 (1997).
[13] H. Morgan *et al.*, J. Phys. D **34**, 1553 (2001).
[14] D. S. Clague and E. K. Wheeler, Phys. Rev. E **64**, 026605 (2001)
[15] M. Washizu, J. Electrost. **29**, 177 (1992).
[16] M. Washizu and T. B. Jones, J. Electrost. **33**, 187 (1994).
[17] T. B. Jones and M. Washizu, J. Electrost. **37**, 121 (1996).
[18] X. Wang, X. B. Wang, and P. R. C. Gascoyne, J. Electrost. **39**, 277(1997).
[19] G. H. Markx, R. Pethig, and J. Rousselet, J. Phys. D **30**, 2470 (1997).